Volume 1 | Number 1 | Jan 2013 | Pages 1–100

Journal of
Materials Chemistry A

Materials for energy and sustainability
www.rsc.org/materialsA

Li⁺

ROYAL SOCIETY OF CHEMISTRY

ROYAL SOCIETY OF CHEMISTRY

www.rsc.org/materialsA

Table of Contents Graphic and Statement for: Jenkins et al. *Systematic electrochemical oxidative doping of P3HT to probe interfacial charge transfer across polymer-fullerene interfaces*

Manuscript ID TA-ART-08-2014-004319
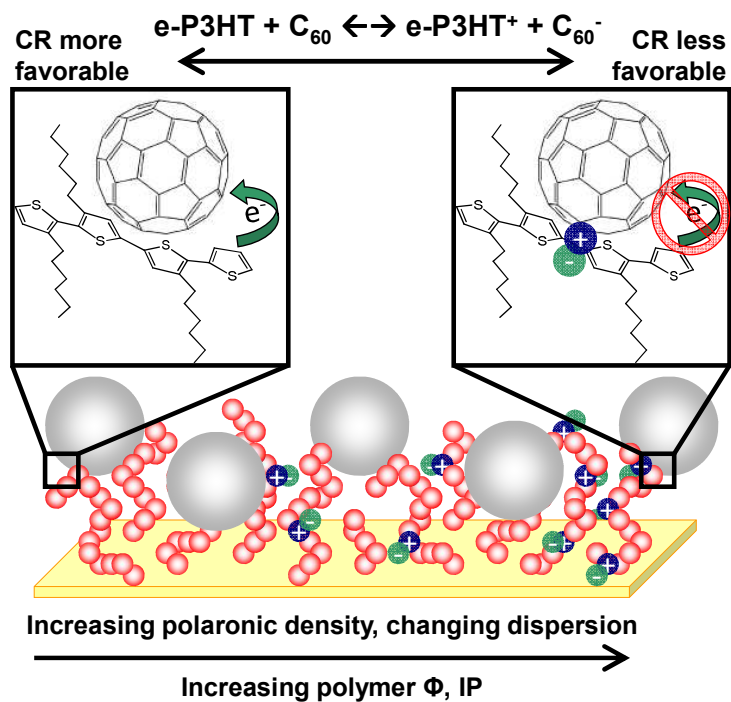
Control of charge redistribution across e-P3HT/C_{60} interfaces is accomplished through the systematic electrochemical oxidation of the thiophene species.

Journal Name

ARTICLE

Systematic electrochemical oxidative doping of P3HT to probe interfacial charge transfer across polymer-fullerene interfaces

Judith L. Jenkins,[a,b] Paul A. Lee,[a] Kenneth W. Nebesny[a] and Erin L. Ratcliff*[c]

This work demonstrates the detection and control of interfacial charge transfer across polymer-fullerene interfaces relevant to organic electronic platforms, including solar cells and photodetectors. Electrochemical deposition of poly(3-hexylthiophene) (e-P3HT) and subsequent electrochemical oxidation to systematically vary the fraction of oxidized thiophene (e-P3HT$^+$) was used to form donor polymer films. The fullerene electron acceptor C_{60} was vacuum deposited onto the e-P3HT, and interfacial interactions were monitored with optical and photoelectron spectroscopy. Charge redistribution (sub-stoichiometric or even stoichiometric electron transfer) from e-P3HT to C_{60} was observed when the initial fraction of e-P3HT$^+$ was low, as evidenced by the formation of new polaronic species and simultaneous n-doping the C_{60}. These charge transfer results are expected to impact interfacial rates of free carrier generation and recombination, as well as competing charge transport processes, particularly in thin film devices (< 60 nm). While charge transfer of this sort has been previously observed, the ability to control the extent of charge redistribution through the systematic oxidation of the thiophene species demonstrates additional chemical tunablity that can further increase the functionality of polymer/fullerene type II heterojunctions. Collectively, this work highlights the need to characterize and strategically manipulate nanoscale deviations from bulk properties in the future rational design of functional organic electronics.

Introduction

A wide range of organic electronic platforms rely on charge transfer processes across dissimilar organic-organic interfaces. One of the most-studied organic-organic interfaces is that formed between a conducting polymer electron donor (D) and a fullerene electron acceptor (A) for use in solar cell and photodetector applications. In these platforms, a photoinduced electron transfer across the D/A interface results in the generation of free carriers useable current for work or as an analytical signal. The chemical functionality of a D/A heterojunction depends strongly on many (often competing) macroscale characteristics, including the optoelectronic properties of D and A materials, such as energy levels and optical band gaps. These bulk properties of individual materials are relatively straightforward to measure and synthetically control, as evidenced by the near-exponential growth in organic photovoltaic (OPV) photoconversion efficiency in the last decade. However, the local, molecular-level deviations from these bulk properties still limit devices built around organic-organic interfaces. These deviations are often difficult to detect and strategically control, especially those occurring directly at the D/A interface in solution-processed layers, where precise control over the interfacial chemistry is critical for the realization of efficient functionality in organic electronic devices.

The local electronic interactions that occur when the polymer and fullerene come into contact with one another are of great importance when considering electronic functionality.[1] Both Zhu et al.[1q] and Bredas et al.[1a] advocate for the electronic equilibrium process depicted in Equation 1,

$$D + A \longleftrightarrow D^{\delta+} + A^{\delta-} \longleftrightarrow D^{+\cdot} + A^{-\cdot} \qquad (1)$$
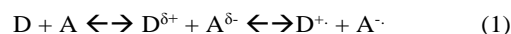
where electrons in the highest occupied molecular orbitals of the donor polymer may undergo sub-stoichiometric or even stoichiometric electron transfer to the fullerene lowest occupied molecular orbitals spontaneously in the ground state or when a thermal activation energy barrier is overcome. Interfacial charge redistribution (partial or even complete charge transfer to establish local electronic equilibrium at the interface) of this nature can result in band-bending, changes in the interfacial trap state density, interface dipoles, and spatially confined charge transfer complexes at the interface; the extent of charge redistribution at the D/A interface often depends critically on (or may significantly alter) the local density of states.[1f, 1n, 1q, 2] Understanding interfacial interactions is further complicated when considering polymers versus small molecules, where distributions of conjugation lengths and polymeric microstructure give rise to trap states and/or a broad density of states tailing into the bandgap. Ultimately, the discrete frontier orbital energies measured for bulk materials in isolation may not account for ground state interactions resulting from charge redistribution, which are themselves difficult to predict, difficult to control, and therefore must be measured.[1a, 1q]

We have recently introduced photoactive, electrodeposited poly(3-hexylthiophene) (e-P3HT) ultra-thin films, grown on indium-tin oxide (ITO) substrates, which can function as a rectifying type II heterojunction with thin films of the electron acceptor, C_{60}.[3] The unique electrochemical procedure used to

generate these films has been described in detail elsewhere and results in energetically highly disordered films.[3a] After deposition, the e-P3HT film can be oxidatively doped as desired (e-P3HT → e-P3HT$^+$ + e$^-$) using potential control under chronoamperometry conditions. This electrochemical oxidative doping procedure controllably and reproducibly generates polaronic and bipolaronic e-P3HT, collectively referred to as e-P3HT$^+$, without the use of dopants that require specific energy level alignment to facilitate charge transfer and oxidize the polymer. Introducing e-P3HT$^+$ is analogous to increasing the hole density and altering the energetic distribution of charge carriers throughout the polymer film; further discussion is given in the SI section. Increased hole density has been reported to increase the polymer ionization potential,[3a] which in turn can affect the magnitude of the energetic barrier to interfacial charge redistribution when interfaced with an acceptor material, as depicted in Figure 1. Likewise, introducing additional P3HT$^+$ units is expected to alter the hole mobility of the material, although comparing transport effects is beyond the scope of this work.

There are several key advantages to using this electrodeposited polymer system in conjunction with vacuum-deposited C_{60} to monitor interfacial charge redistribution at an organic-organic interface. First, both e-P3HT and e-P3HT$^+$ have discreet chemical signatures; any changes in the polymeric hole density resulting from interfacial charge redistribution can be followed spectroscopically. Second, while the polymer electrodepostition method does not yield the high molecular weight, regioregular P3HT commonly used in polymer/fullerene OPVs, we are able to systematically control and precisely track relatively high hole densities in these disordered films (up to 45 % of the thiophene rings oxidized without chemically reactive additives). Third, electrodeposition can afford ultrathin e-P3HT films (ca. 10 nm) which, when interfaced with sub-monolayer coverages of C_{60} in a planar bilayer geometry, effectively model domain sizes relevant to optimized blended heterojunction OPV architectures. Finally, the ability to electrochemically synthesize, deposit, and control oxidative doping (and energy levels) of a conducting polymer has broader applications for organic electronics, such as for charge-selective interlayers, variable carrier density polymeric contacts, usage with non-planar substrates, and fabrication of large bandwidth photodetectors, where response speeds are dependent on carrier transit times associated with thicknesses and controlled mobilities. Electrodeposition processes could also enable the use of more environmentally friendly solvents than those commonly used in other wet deposition techniques, as electrodeposition does not rely on the solubility of the polymer, but only that of the monomer.

In this work, we show that by controlling the percentage of oxidized e-P3HT$^+$ in the polymer film (and ultimately, at the D/A interface), we can systematically vary the interfacial charge redistribution between the polymer and vacuum deposited C_{60}, as monitored by changes in core level photoemission of the buried interface. As an example of the importance of D/A interfacial chemistry, we correlate these controllable charge redistribution events at the buried e-P3HT/C_{60} interfaces to the realized V_{OC} in OPVs built from e-P3HT/C_{60} heterojunctions, demonstrating the link between interfacial energetic disorder and experimentally observed macroscopic parameters (SI1).[4]
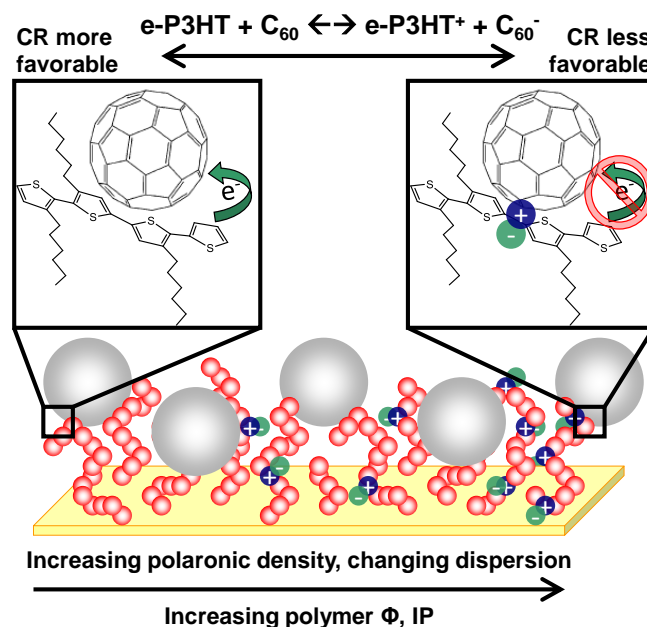
Figure 1: Cartoon of the polymer-fullerene interfaces discussed in this work. The polymer, e-P3HT (red balls) can be systematically oxidized (blue circles, +) retaining the PF_6^- counter ion (green circles, -), and C_{60} (grey balls) is vacuum deposited onto the polymer film. Charge redistribution (CR) across the e-P3HT/C_{60} interface (expanded squares) is controlled by the initial percentage of oxidized e-P3HT because oxidizing the polymer changes its work function (Φ), ionization potential (IP), and local dispersity.

We suggest that electrochemical oxidative doping can be used to strategically facilitate or inhibit charge transfer/redistribution across D/A interfaces to afford the desired chemical functionality in increasingly efficient future organic electronic platforms beyond the use of this system solely in OPVs.

Experimental

Chemicals

3-hexlythiophene (3-HT), 3-thiophene acetic acid (3-TAA), and 57% hydriodic acid in water were used as purchased (Aldrich). Tetrabutylammonium hexafluorophosphate (TBAPF$_6$) (Aldrich) was recrystallized once from ethanol prior to use. All solutions were made with UV-grade acetonitrile (Honeywell) and were thoroughly de-oxygenated with Ar(g) prior to electrodeposition. Bathocuprine (BCP) was purchased from Aldrich, fullerene (C_{60}) was obtained from MER, and these chemicals were purified by multiple entrainer sublimation prior to use. Indium tin oxide (ITO) on glass was purchased from Colorado Concept Coating LLC, with a film thickness of ~100 nm and a sheet resistance of ~15 ohm/square. The ITO was cut into ~ 1-inch squares, detergent-solvent cleaned, acid-activated, and functionalized with 3-TAA as previously described.[5]

Electrodeposition and electrochemical oxidative doping

ITO substrates modified with 3-TAA served as the working electrode in a 3-electrode electrochemical cell where the counter electrode was detergent-cleaned ITO and the reference electrode was Ag|AgNO$_3$ (10 mM). The cell was filled with a monomer solution consisting of 3-HT (0.01 M) and TBAPF$_6$ (0.1 M) in acetonitrile. Using a CHI 660 potentiostat (CH Instruments, Austin, TX), the potential was stepped to +1.40 V for 0.5 s to

initiate the oxidation of the surface confined 3-TAA and initiate 3-HT oxidation and oligomerization in solution region adjacent to the ITO electrode.[6] The potential was then immediately stepped to +1.35 V (vs. Ag/AgNO₃ (10 mM)), where polymer electrodeposition onto the ITO substrate occurred until the desired polymer film thickness was achieved. Thickness was monitored by the current passed during electrodeposition. All e-P3HT films used for XPS/UPS characterization and in fabrication of bilayer devices were ~25 nm thick yielding an electrodeposition charge of ca. 6 x 10^{-3} C/cm². The monomer solution was then replaced by an electrolyte-only solution (0.1 M TBAPF₆ in acetonitrile). The potential was stepped to the desired oxidation potential for 60 s. Undoped films were oxidized at +0.00 V, partially doped films were oxidized at +0.60 V, and highly doped films were oxidized at +1.00 V versus Ag|AgNO₃ (10 mM). Films were removed from potential control while still at the specified oxidation potentials, thoroughly rinsed with acetonitrile, blown dry with N₂ (g) and transferred to high vacuum for spectroscopic analysis or solar cell construction.

Photoelectron spectroscopy

X-ray and UV-photoelectron spectroscopy were performed with a Kratos Axis Ultra X-ray photoelectron spectrometer with a monochromatic Al Kα source (1486.6 eV) for XPS measurements and a He(I) excitation source (21.2 eV) for UPS measurements, all at a base pressure of 10^{-9} torr. Photoelectrons were collected in a hemispherical analyzer and detected with a photodiode array. A -9.00V bias was applied to the sample to enhance collection of the lowest kinetic energy electrons during UPS analysis. C₆₀ was thermally evaporated in adjacent chamber without breaking vacuum in nominal 0.3 nm increments (deposition rate of 0.06 Å/s) as calibrated by AFM and measured by quart crystal microbalance (Newark, 10 MHz) and a homebuilt frequency monitor. All XPS spectra were collected at a ~60° incident angle to enhance surface sensitivity. The resulting XPS binding energies were corrected to the alkyl C 1s feature at 284.6 eV and were fit as Gaussian peaks with linear baseline correction. All UPS spectra were referenced to the Fermi level, E_F, of a clean polycrystalline gold substrate.

Results and Discussion

1. Control of the percentage of oxidized polymer using electrochemical oxidative doping

Prior to studying the e-P3HT/C₆₀ interfacial interactions, control over the optical, chemical and electronic properties of the e-P3HT films as a function of oxidation of the polymer is illustrated in Figure 2. The chemical signatures of the polaronic and bipolaronic e-P3HT (e-P3HT⁺) will later be used to follow interfacial charge redistribution at e-P3HT/C₆₀ heterojunctions, so thorough characterization of e-P3HT in the absence of C₆₀ is critical. We will refer to oxidized thiophene species as "dopants," as an increase in the amount of electrochemically oxidized thiophenes is synonymous with an increasingly p-doped polymer film.

Figure 2a shows a cyclic voltammogram of the electrodeposited P3HT film, with respect to 0.01 M Ag|AgNO₃. At low oxidation potentials (<0.2 V), there is little faradaic current and the polymer is predominantly in a neutral or undoped form, similar to what would be expected for as-cast polymer films typically used in organic photovoltaics.
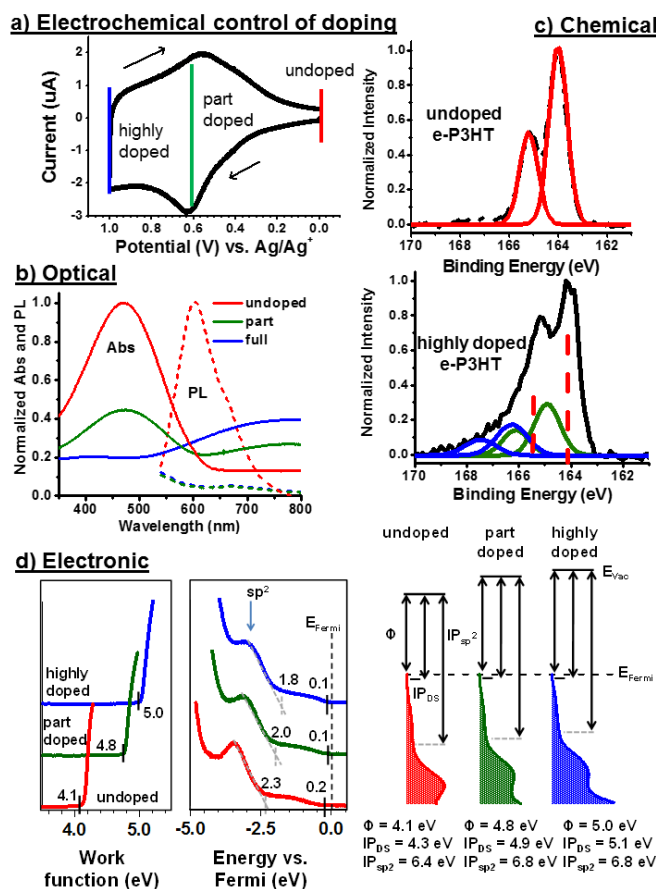
Figure 2. Demonstration of the control over optical, chemical, and electronic properties of the electrodeposited P3HT (e-P3HT) film. (a) Cyclic voltammogram of e-P3HT film in 0.1 M TBAPF₆ in acetonitrile, with respect to 0.01 M Ag|AgNO₃. Three regions of interest are identified, where the polymer is in an undoped (0.0 V), partially p-doped (0.6 V) and highly p-doped (1.0 V) state. (b) Optical properties (absorbance and photoluminescence) of solid state e-P3HT films with respect to the three regions identified in (a). (c) X-ray photoelectron spectroscopy of the raw (black lines) and fit (colored lines) of the S 2p doublet structure of the e-P3HT in the undoped (top) and highly doped (bottom) state. The undoped polymer can be fit with a single doublet (top), while the highly oxidized polymer shows two additional doublets at higher binding energies corresponding to the polaronic and bipolaronic thiophene species (bottom). (d) The electronic properties of e-P3HT as a function of polaronic density as evaluated with UPS. Data show changes in work functions (Φ, left panel), valence features and ionization potentials (IP, middle panel) and energy band diagrams (right panel) as the polymer is increasingly doped.

As the potential is swept towards more positive potentials, the e-P3HT is oxidized to generate e-P3HT⁺, as evidenced by the (negative) faradaic current. The potential range over which the polymer oxidation occurs approximates the density of states within the polymer HOMO-like feature; we anticipate that the change in the occupied density of states that occurs with electrochemical doping will impact the charge transfer at the interface with the fullerene. The most easily oxidized thiophene rings yield the current at voltages just positive of 0.2 V, while the current at increasingly positive potentials comes from thiophene rings that are energetically more difficult to oxidize.

It is important to note that this oxidation is reversible, as evidenced by the reverse (reduction) current.

By holding the polymer film at a particular potential until faradaic current is exhausted (demonstrating no more exchange of electrons), we are able to oxidize the polymer-modified electrode to a static state, with a specific doping density associated with the fraction of oxidized polymer. Our previous work has demonstrated the ability to vary the location (surface or buried) and fraction of doped polymer using different applied potential functions.[3a, 3b] We have chosen to focus this study specifically on three main doping densities with respect to applied oxidizing potential: undoped (0.0 V); partially doped (+0.6 V); and highly doped (+1.0 V).

In Figures 2b-d, the optical, chemical, and energetic impact of different degrees of electrochemical oxidation (changes in density of states distributions with p-doping) are referenced with respect to the three regions of interest identified in Figure 2a. Figure 2b shows the absorbance (solid lines) and photoluminescence (dashed lines) of the polymer film with successive electrochemical oxidation. Potential-dependent e-P3HT absorbance and photoluminescence spectra (SI2) show that the oxidative doping can be fine-tuned over a 1 V range. The spectra of the e-P3HT films in air (Figure 2b) show that the e-P3HT$^+$ species formed through electrochemical oxidation persist after the films are removed from potential control. It is important to note that these films showed minimal change in absorbance over several hours despite being exposed to air. This is an important material processing distinction from p-doping using chemical oxidizers (additives), which can react with oxygen. The electrodeposited films are very loosely packed relative to the lamellar stacking observed in annealed regioregular P3HT films.[3a, 3b, 7] The increased disorder and lower regioregularity of the e-P3HT films, relative to regioregular P3HT (SI2), is evident from the absorbance spectrum of the undoped polymer film in Figure 2b (red).[8] The maximum absorbance of the π-π* transition near 480 nm is blue-shifted, and the spectra do not contain the fine structure commonly associated with regioregular P3HT (specifically shoulders at 560 nm and 605 nm).[7] We attribute the differences in the absorbance spectrum to the physical disorder resulting from the electrodeposition process, where 3-HT monomers in solution are oxidatively polymerized in the presence of solvent and electrolyte molecules

As the film is oxidatively doped, the peak at 480 nm corresponding to undoped e-P3HT decreases in intensity, while the polaronic and bipolaronic features red of 600 nm appear (collectively referred to as e-P3HT$^+$). The photoluminescence spectra also illustrate the achieved electrochemical oxidative doping (Figure 2b, dotted lines); a decrease in PL intensity with increased polaronic density is observed, with quenching previously attributed to the presence of polarons.[9] The optical changes associated with the presence of polaronic species are a key a chemical signature with which to further probe effective hole densities and resulting energetics.

X-ray photoelectron spectroscopy (XPS) can be used to quantify the relative percentage of e-P3HT$^+$ to neutral e-P3HT achieved through electrochemical oxidation, with the S 2p core line shapes for two different oxidation fractions shown in Figure 2c. All XPS spectra were collected at a surface-sensitive 60° take-off angle, with core electrons collected from approximately the top 2 nm of the polymer film. Differences in S 2p line shapes, arising from the polaronic states of the polymer film, are clear in the comparison of the undoped (Figure 2c, top) and highly doped (Figure 2c, bottom) e-P3HT films. Details of the assignments of these peaks are given in prior publications.[3a, 3b] The undoped e-P3HT spectrum is fit with a Gaussian doublet in a 2:1 ratio, where the S $2p_{3/2}$ and S $2p_{1/2}$ peaks spaced by 1.2 eV have binding energies of 164.0 eV and 165.2 eV respectively. When the polymer is electrochemically oxidized, the S 2p spectra show clear evidence of peak broadening, with the presence of a tailing feature in the high binding energy region (165 to 168 eV). This shoulder feature can be fit with doublets associated with polarons (S $2p_{3/2}$ at 164.9 eV, S $2p_{1/2}$ at 166.1 eV) and bipolarons (S $2p_{3/2}$ at 166.3 eV, S $2p_{1/2}$ at 167.5 eV).[3a] Elemental fits of the S 2p spectra in the SI section yield approximately 5%, 35%, and 45% of the total thiophene rings sampled are oxidized for e-P3HT films oxidized at 0.0 V, +0.6 V and +1.0 V vs. Ag|AgNO$_3$, respectively. Complimentary C 1s spectra suggest similar polymer oxidation percentages as a function of doping potential as demonstrated in our previous work (SI3).[3a, 3b]

In the partially doped and highly doped e-P3HT, XPS revealed detectable fluorine signal, corresponding to the PF$_6^-$ counter ion retained in the film during electrochemical oxidation (SI3). No evidence of fluorine was observed in the undoped e-P3HT. As expected, increased oxidation of the polymer film results in increased counterion intercalation, previously demonstrated to be buried within the polymer film and not confined directly at the surface of the oxidized e-P3HT.[3a, 3b] The retained electrolyte is assumed to enable such high doping (>20%) in our polymer films through Coulombic stabilization. Analogous to our previous works, the F 1s to S 2p peak ratios can also be used to determine relative changes in doping percentages of the polymer films (with the appropriate sensitivity factors). These ratios are given in SI3 and indicate similar doping percentages in the partially and fully doped e-P3HT films as those obtained from fits of the S 2p spectra discussed.

Changes in the hole density with respect to electrochemical oxidation potential are reflected in the effective work function (Φ) and ionization potential (IP$_{e-P3HT}$) in Figure 2d, as measured using ultraviolet photoemission spectroscopy (spectra data given in the left and center panel of Figure 2d). Complete UPS spectra of the different doped polymer films are given in the SI Section 4. In the left panel of Figure 2d, we readily observe that increasing the percentage of oxidized thiophene (e-P3HT$^+$) increases the p-doping character of the polymer, increasing in the work function (Φ) from 4.1 eV for the neutral e-P3HT (bottom spectrum) to 5.0 eV for the highly oxidized e-P3HT (top spectra). The surface vacuum change (as demonstrated in the difference in the work function) reflects a change in surface dipole consistent with increasing polaronic density (surface) and PF$_6^-$ counterions (buried) in the interfacial region.[3b] The center panel of Figure 2d shows the valence region of the polymer film, with energy reported with respect to the Fermi level (E$_{Fermi}$ at 0.0 eV). In all three cases, we observe two distinct feature regions. The first is a Gaussian-like peak with a local maximum, which has previously been attributed to the sp^2 hybridized orbitals of the thiophene unit;[3b, 10] dashed lines have been included to guide the eye to linear fits for the onset of each of these features. The neutral film has the most narrow full width half maximum in the density of states for this feature, indicating that the sp^2 hybridized orbitals are generally in the same chemical state (undoped). An increase in the electrochemical doping correlates with both a broadening of the sp^2 feature and a shift in the onset density of occupied states towards the Fermi level. The electrochemical oxidation should likewise result in unoccupied gap states that were previously filled. The increase in the full width half maximum with electrochemical doping suggests that there is a greater distribution of energetic sites within the doped polymer film, consistent with 35% and 45% of the monomer units being

oxidized for the partially and highly doped films, respectively. The second feature, at 0.1 to 0.2 eV below the Fermi level, has previously been attributed to defect states within the polymer.[3b] We expect that these defect states (DS) and the newly introduced unoccupied states will play a critical role in interfacial alignment with C_{60} acceptor molecules. Likewise, interfacial charge transfer is expected to influence rates of free carrier generation and/or recombination and transport, although specific mechanisms are beyond the scope of this work.

The right panel of Figure 2d gives the interpreted energy band diagrams from the UPS spectra. The work function is defined as the energetic difference between the local surface vacuum level (E_{VAC}) and the Fermi level of the surface. Ionization potentials are determined from the difference in energy between the onset density of states feature and the surface vacuum level. Ionization potentials for both the sp^2 feature (IP_{sp2}) and the defect sites (IP_{DS}) features are given as a function of electrochemical oxidative doping. From the energy band diagram, it can readily be observed that oxidizing a fraction of the polymer removes electrons from the top of the valence band. As such, oxidation is expected to result in the creation of new unoccupied states, and shifting the Fermi level closer to the remaining occupied states. For reference, the ionization feature for regioregular P3HT is typically ~4.7 eV, taken from the onset of the first observed feature in the density of states.[1c, 1d]

2. Interfacial charge redistribution at the e-P3HT/C_{60} interface

We anticipate that the fraction of e-P3HT$^+$, varied systematically with electrochemical oxidative doping, will strongly influence the interfacial charge redistribution occurring when e-P3HT comes into contact with an acceptor (i.e.C_{60}), as depicted in Figure 3. Changing the fraction of oxidized species effectively changes the ionization potential of the most easily oxidized electrons in the polymer accessible for charge transfer at the interface with C_{60}. The difference between the polymer ionization potential and the fullerene electron affinity (ΔE_{DA}) approximates the energetic barrier to charge redistribution. However, ΔE_{DA} barrier for these systems seems prohibitively large for ground state charge transfer from the polymer HOMO to the fullerene LUMO. We hypothesize that charge redistribution may proceed through shallow trap/defects near the polymer and/or fullerene valence bands. When the polymer remains in the neutral state, corresponding to undoped e-P3HT, some redistribution of electron density from the polymer to the fullerene is expected (Figure 3, left panel). Increasingly oxidizing the film increases the ionization energy, which may ultimately increase the energetic barrier to redistribution (assuming vacuum level alignment). However, the PF_6^- counter ions retained during electrochemical oxidative doping stabilize polarons generated during the electrochemical doping and may lead to a more energetically favorable pathway for formation of polarons through interfacial charge redistribution. Excessive oxidative doping of the polymer film could result in a back electron transfer from the C_{60} to the polymer, ultimately reducing the p-type character of the film when the interface is formed with C_{60}.

undoped/C_{60}   **partially/C_{60}**   **highly/C_{60}**

Increasing polaronic density

(decreasing interfacial charge redistribution)
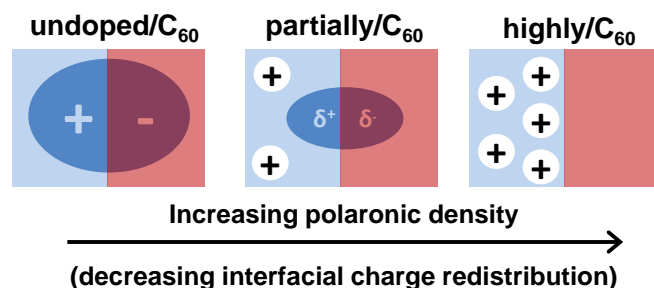
Figure 3. Qualitative description of the importance of interfacial alignment between the polymer and fullerene (C_{60}) as a function of p-type doping. When the hole density is low (left) corresponding to undoped e-P3HT, some redistribution of electron density from the polymer to the fullerene is expected, but as the hole density increases (center, right), the energetic barrier to redistribution is expected to increase and less interfacial charge redistribution is expected.

Thus, energy levels of the polymer and the fullerene directly at the polymer-fullerene interface cannot be assumed to reflect bulk energies and must be measured.[1a]

This section will focus specifically on charge reorganization at the e-P3HT/C_{60} buried interface as a function of oxidation of the polymer. We specifically refer to this proposed mechanism as charge reorganization, because we can only follow what is happening in the polymer and are unable to spectroscopically resolve the presence of C_{60}^- because of the highly delocalized nature of the molecular orbitals of the fullerene. Likewise, we cannot precisely determine the energetic position of the polymeric and fullerene states (surface/gap/defect) through which the charge transfer processes occur.

We first follow the interfacial processes optically, through photoluminescence, post deposition of the C_{60} layer. Then we compare changes in the chemical environment, monitored via core S 2p spectra for the different films, with focus on changes in the degree of oxidized species at the buried interface. Finally, we correlate the optical, chemical, and energetic changes occurring with C_{60} deposition. By monitoring the different optical, chemical, and electronic changes occurring directly at the e-P3HT/C_{60} interface, we confirm that electrochemical oxidative doping can be used to strategically facilitate or hinder interfacial charge redistribution across D/A interfaces.

2.1 Optical properties of the e-P3HT/C_{60} interface

Photoluminescence (PL) has been used extensively to monitor interfacial interactions in polymer/fullerene heterojunctions,[11] although the exact chemical nature of the interfacial interactions is still debated. While quenched PL can suggest interfacial charge redistribution, the detection of quenching does not automatically confirm that full electron transfer from e-P3HT to C_{60} occurs at the e-P3HT/C_{60} heterojunction. Ohkita et al.[11d] showed that PL quenching can occur even when there is not complete charge transfer at a type II heterojunction. After separately calculating free energy changes (ΔG) for PL quenching and for charge transfer, it was apparent that the ΔG corresponding to PL quenching at polymer/fullerene heterojunctions was significantly smaller than the ΔG required for complete charge separation. Still, quenching of the PL at the polymer/fullerene interface implies some degree of electronic equilibration between the donor and the acceptor.

C_{60} was vacuum deposited onto the polymer films through a shadow mask and PL images were collected through an inverted

fluorescence microscope from the polymer side, allowing visualization of the buried polymer/fullerene interface, as shown in Figure 4. In regions void of C_{60}, the PL intensity of the e-P3HT films in air decreases dramatically with increasing p-type character (increased oxidation fraction). The decrease in PL intensity suggests that photogenerated charges in neutral regions of the film are quenched by the neighboring polaronic species, consistent with lower PL with increased p-doping in Figure 2b.[12] From the PL spectra and images of the e-P3HT/C_{60} heterojunctions, it is evident that the polymer PL is also quenched significantly when C_{60} comes into contact with the undoped e-P3HT film. The undoped e-P3HT film in Figure 4a shows fluorescent e-P3HT next to the dark circles corresponding to regions of C_{60}. This quenching is less apparent in the partially doped and highly doped e-P3HT films (Figures 4b and 4c), likely due to their already low PL intensities.

2.2 Chemical composition of the e-P3HT/C_{60} interface

In order to evaluate the potential charge redistribution (sub-stoichiometric or even stoichiometric charge transfer) at the e-P3HT/C_{60} interfaces as a function of electrochemical oxidation, as suggested by the PL images (Figure 4), we measured changes in the C 1s and S 2p XPS spectra as a function of polymer doping and C_{60} coverage. We hypothesize that electron transfer from the C_{60} to the e-P3HT may change the core level energies directly at the interface, giving chemical evidence for interfacial charge redistribution. (e-P3HT + C_{60} → e-P3HT$^+$ + C_{60}^-) A complete discussion of the fitting procedure and corresponding fits for all C 1s and S 2p spectra are given in the SI Section 3. Analysis of the S 2p spectra for the partially doped e-P3HT film as a function of C_{60} thickness is described here.

Figure 5a gives the S 2p core level line shapes (background corrected) for the partially doped e-P3HT with incremental depositions of C_{60}; similar plots for other polymer doping densities are given in the SI section. These spectra were fit with three doublets corresponding to neutral thiophene (S $2p_{3/2}$ = 164 eV, S $2p_{1/2}$ = 165.2 eV), as well as the polaronic thiophene and the bipolaronic thiophene (BE ca. 165 -167 eV). These binding energies are consistent with those used in Figure 2b, and doublets corresponding to the neutral and polaronic thiophene species are overlain on Figure 5b. From our previous results[3a, 3b] and the results presented in Figure 2, monitoring only the S 2p line shape changes is consistent with also monitoring the ratio of S 2p to F 1s signal, when available. While the C 1s spectra do reflect small changes in the about of oxidized carbon with charge redistribution (SI3), it is difficult to separate contributions from the polymer and the fullerene in these spectra. Thus, the S 2p spectra are used here to follow changes in polymer oxidation due to charge redistribution.
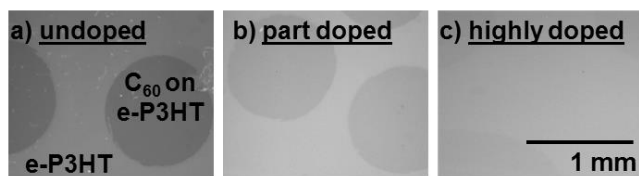
Figure 4. Photoluminescence images for the e-P3HT/C_{60} heterojunctions (a-c) were collected from the polymer side in air using an inverted fluorescence microscope and allow visualization of the buried e-P3HT/C_{60} interface. Polymer PL is quenched by C_{60} (circles) for the undoped (a) and partially doped (b) polymer films.
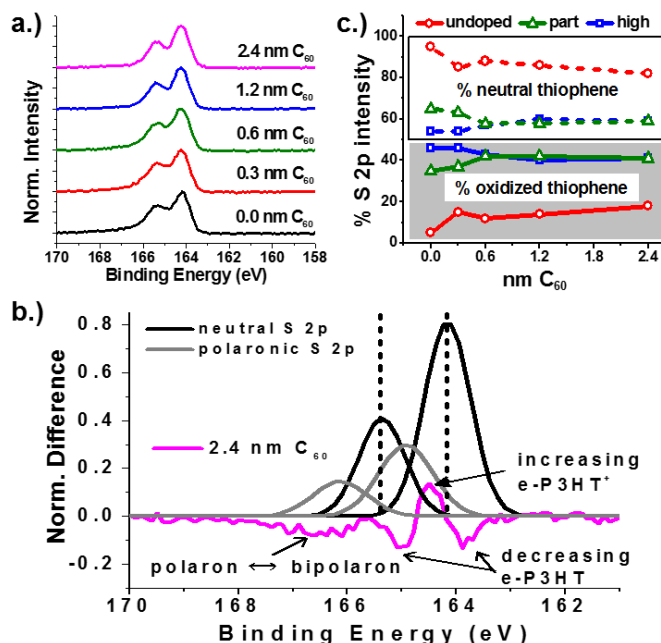
Figure 5. The S 2p XPS spectra (a) for the partially doped e-P3HT film as C_{60} is deposited show changes in the polymer doping. The red spectrum is the polymer by itself, and the additional spectra are the polymer after increasing amounts of C_{60} are deposited onto the polymer film. A difference spectrum (b), where the partially doped e-P3HT spectrum was subtracted from the e-P3HT/C_{60} spectra, highlights the increase in polaronic density when C_{60} is deposited on the partially doped polymer. Gaussians overlayed on the difference spectrum represent the neutral S 2p doublet (black) and the polaronic S 2p double (grey). There are decreases in photoemission intensity coming from neutral sulfur (lower BE), and increases in signal at higher binding energies, suggesting an increase in polaronic density as the e-P3HT came into contact with the C_{60}. The negative signal at higher binding energies suggests re-equilibration of the polaronic and bipolaronic e-P3HT species as interfacial charge transfer occurs. These spectral changes are consistent with partial electron transfer into the C_{60} as described in Figure 3. Changes in interfacial polaronic density (c) show that the undoped and partially doped e-P3HT films are doped by C_{60}, while the highly doped e-P3HT film is slightly de-doped.

Changes in the binding energies of core S 2p electrons with the addition of C_{60} are subtle in Figure 5a, although an increase in the overall width of the S 2p spectrum with increasing C_{60} is observed. Visualization of the small differences are facilitated via differential spectra in Figure 5b, which are obtained by the subtraction of the polymer-only normalized spectrum from the normalized spectrum of e-P3HT + C_{60}. Black dotted lines corresponding to the maxima of the neutral thiophene doublet guide the eyes. There is an increase in the photoemission signal from polaronic states (higher BE) when C_{60} is deposited on the partially doped e-P3HT film and a corresponding decrease in the signal from neutral thiophene species (BE 164 eV). These spectral changes indicate interfacial charge redistribution depicted in Figure 3 yielding newly-formed, polaronic e-P3HT$^+$, although the magnitudes of the intensity changes suggest that little more than the near interfacial layer of e-P3HT is affected by this electronic redistribution of charges at the interface in order to achieve equilibrium. It is important to note that this is

an increase in the e-P3HT⁺ fraction beyond that initially afforded by electrochemical oxidative doping.

Figure 5c shows the changes in interfacial oxidized polymer fraction (quantified from the spectral fits in SI3) as C_{60} is deposited onto either the undoped, partially doped, or highly doped e-P3HT films. Solid lines map the changes in the % of oxidized thiophene at the interface, while the dotted lines track changes in the percentage of neutral thiophenes. Both the undoped and partially doped e-P3HT exhibit increases in oxidized sulfur species, likely due to some electron transfer from the polymer to near-valence, unoccupied states in the fullerene. Conversely, the fraction of oxidized thiophene components decreased slightly with the addition of C_{60} to the highly doped e-P3HT film (highest ionization energy film), suggesting a slight reduction of the polymer. We suggest that this reduction may result from partial electron transfer from the C_{60} to the e-P3HT⁺ and/or some re-equilibration of the e-P3HT⁺ near the interface. Similar trends were observed in the C 1s spectra (SI3). We were unable to spectroscopically resolve the presence of C_{60}^{--}, presumably because of the low abundance and the signal overlap with other C 1s spectral features and because of the highly delocalized nature of the molecular orbitals of the fullerene.

As stated previously, the retention of electrolyte anion is unique to the electrochemical deposition and doping procedures used to generate e-P3HT films and is not present in spin-coated regioregular P3HT nor in vacuum deposited films of other molecular semiconductors. The retained PF_6^- counter ions in the partially doped and highly doped e-P3HT will likely serve to electrostatically stabilize charge redistribution at the interface. However, it is important to note that the largest observed change in fraction of oxidized thiophene occurred at the neutral e-P3HT/C_{60} interface, where no electrolyte was detected. Furthermore, only the S 2p signals were used to track changes in the fraction of oxidized thiophene resulting from charge redistribution in Figure 5 because any changes in the F 1s signal likely do not reflect interfacial charge redistribution. This is supported by the fact that the changes in the fraction of oxidized thiophene did not change the core level energy for the PF_6^- counter anions. While the F 1s peak intensity did change, it is difficult to decouple changes in intensity due to a decreased sampling depth (due to the C_{60} film) and/or counter ion migration to/from the surface with changes in doping. Additionally, previous work on these e-P3HT films suggests that there is a PF_6^- spatial gradient increasing away from the e-P3HT/air interface.[3b] In this work, the F 1s / S 2p ratios decreased with increasing C_{60} thickness (SI3), also likely a reflection of the PF_6^- gradient within the polymer film and the effective decrease in penetration depth. We do expect changes in the polarizability of this interface with C_{60}, depending on the fraction of counterion present and their locations within the e-P3HT film.

2.3 Energetics of the e-P3HT/C_{60} interface

Ultraviolet photoemission spectroscopy (UPS) was used to measure the energy level alignment between the e-P3HT and C_{60}. It is important to note that unlike XPS, UPS spectra do not contain chemical or molecule specific information, and the resulting e-P3HT/C_{60} valence band electronic structure includes contributions from the polymer ionization potential (IP_{e-P3HT}) and the fullerene ionization potential (IP_{C60}). Furthermore, the shifts in the local vacuum level (which defines the surface work function) can arise from interface dipole formation and/or interfacial charge transfer.[2]
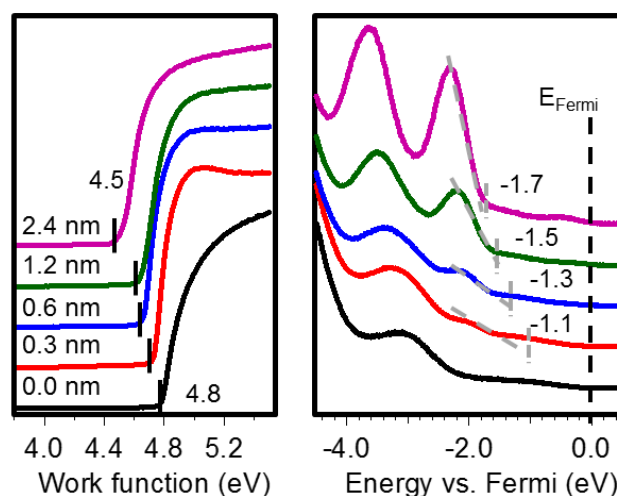
Figure 6. UPS data for the partially doped e-P3HT film (bottom spectrum) with increasing thickness of C_{60} (bottom to top spectra). Left panel shows the onset in the secondary edge, which controls the work function, with increased C_{60} thickness. Right panel shows the evolution in the valence band structure as a function of energy with respect to the Fermi level used to quantitate changes in the heterojunction IP_{C60}, as marked by grey hash-marks.

However, by looking at systematic changes in the energy level alignment between the donor and the acceptor, we can correlate changes in XPS core shifts observed in the e-P3HT with the presence or absence of band bending at the interface to further infer the role of polymer doping density.

Figure 6 shows the UPS spectrum of the partially doped e-P3HT film with successive depositions of fullerene (spectra from bottom to top). The change in the work function is evaluated from the secondary edge onset, as shown in the left panel of Figure 6 and marked with black hash marks. As the thickness of the C_{60} is increased, we observe a decrease in the work function from 4.8 eV for the polymer to 4.5 eV for the fullerene layer. The right panel shows the change in the valence features with the onset density of states indicated by hash marks.

With progressive increase in C_{60} thickness, we see the first and second HOMO features emerge (local maxima at ~2.5 and 3.5 eV, respectively for the 2.4 nm thick C_{60} film) and that the second HOMO peak is slightly broader than the first. There is also a slight change in the onset density of states that tracks with the change in the surface vacuum level. A broadening of the HOMO peaks and a change in the density of states is consistent with previous reports of partially or fully reduced C_{60} (observed via electron transfer between metal atoms and C_{60});[13] however, as stated before, detection of C_{60} anions is beyond the scope of this work. As the C_{60} thickness is increased, the onset density of occupied states moves further from the Fermi level, consistent with an n-type material. Additional UPS spectra for the other polymer/C_{60} heterojunctions and a more detailed description of interpretation can be found in the Supporting Information (SI4).

As previously stated, we expect that the energetic position and density of states of the polymer, controlled via electrochemical doping, will play a major role in the energetics of the heterojunction. Figures 7a-c summarize the work function (upper line, X symbols) and onset density of occupied states (bottom line, closed symbols) taken from the UPS data for the C_{60} on e-P3HT as a function of polymer doping. Energetic differences between the onset density of occupied states and

work function yield ionization potentials (IP). A band gap of 2.4 eV for C_{60} was taken from IPES data[1c, 1d] and assumed to be constant; these values added to the onset density of occupied states to infer electron affinities (EA), as shown by open symbols (middle line in Figures 7a-7c). Fullerene thicknesses above 2.4 nm yielded no further changes to the valence band features (data not shown) or work function.

For all three polymer oxidation states, the work function decreases from that of the polymer-only surface as the fullerene thickness increases. A change in vacuum level suggests the formation of an interface dipole with contributions from the changes in electron density in the fullerene, changes of fraction of oxidized thiophene species at the interface, and the additional polarization of the interfacial e-P3HT. However, a decrease in work function is counter-intuitive to the hypothesized charge transfer and seemingly contradictory to results obtained on similar systems. For instance, both Osikowicz et al. and Guan et al. saw work function increases of 0.5 eV when C_{60} was deposited onto P3HT.[1c, 1r] It is important to note that the amorphous e-P3HT films used in this work are structurally and energetically disordered relative to highly crystalline regioregular P3HT used in the works referenced above. A growing body of research suggests that interfacial disorder can significantly impact the energetics of polymer/fullerene interfaces. Recent work by Castet et al. shows that site-specific differences in polymer/fullerene orientations as well as polarization of the surrounding media contribute to local variations in the frontier orbital energies of the interfacial species.[14] Changing the amount of oxidized thiophene electrochemically may also significantly affect the resulting interfacial microstructure of the e-P3HT/C_{60} heterojunction, and we expect additional polarizability in our doped e-P3HT films due to the incorporation and spatial distribution of the PF_6^- counter ions. It is plausible that charge redistribution which increases the electron density on the fullerene side of the interface may also significantly alter the polarization within the polymer due to shielding effects. Given that UPS is a macroscopic measurement, the observed decreased work functions in our work reflect a surface dipole averaged over a wide range of local microstructure and surface sites, with contributions from discreet polymer/fullerene environments and from the polarizable surrounding media. While the precise reason for the disparity in the work function shift in our work, relative to current literature, is beyond the scope of this work, it does suggest that there is still more to be learned about energetic alignment at organic/organic' interfaces, particularly with respect to doping and local microstructure.

While the deconvolution of the work function is difficult, the ionization potentials, assumed to be associated with the fullerene valence energies, trend towards those of bulk C_{60} (~6.2 eV),[1c, 1d] although the energetic difference between the onset density of states and the Fermi level is different. It is important to note that for each interface, the final work function of the thickest C_{60} film is different. Differences between the onset of occupied states and the Fermi level indicate that charge redistribution has occurred, as a function of the polymer oxidation fraction. If electron transfer from an occupied state of the polymer into to the C_{60} occurs, the Fermi level is expected to move closer to the LUMO of the C_{60} (more n-type). Conversely, C_{60} would be more p-type when electron transfer occurs from the HOMO of C_{60} into polymer, and the Fermi level of the C_{60} layer will move closer to the HOMO.

The UPS data in Figures 7a-7c clearly demonstrate changes in the fraction of occupied and unoccupied states of the C_{60}, that tracks with the initial oxidized fraction of the e-P3HT substrate and observed changes in e-P3HT$^+$ from the XPS in Figure 5. For example, for the undoped film, we observe the largest difference between the Fermi level and the IP of the C_{60} (2.1 eV at 2.4 nm thickness of C_{60}), suggesting that for C_{60} on neutral e-P3HT, the Fermi level is closest to the LUMO of the C_{60}. Likewise, in Figure 5, for the undoped film, we observed a large change from minimal degree of oxidized species to almost 20% of the film being oxidized. The energetic difference between the Fermi level and occupied states decreases to 1.8 eV for the partially doped film and to 1.4 eV for the highly doped e-P3HT film, meaning the Fermi level moves closer to the HOMO of the C_{60} with increasing polymer oxidation.
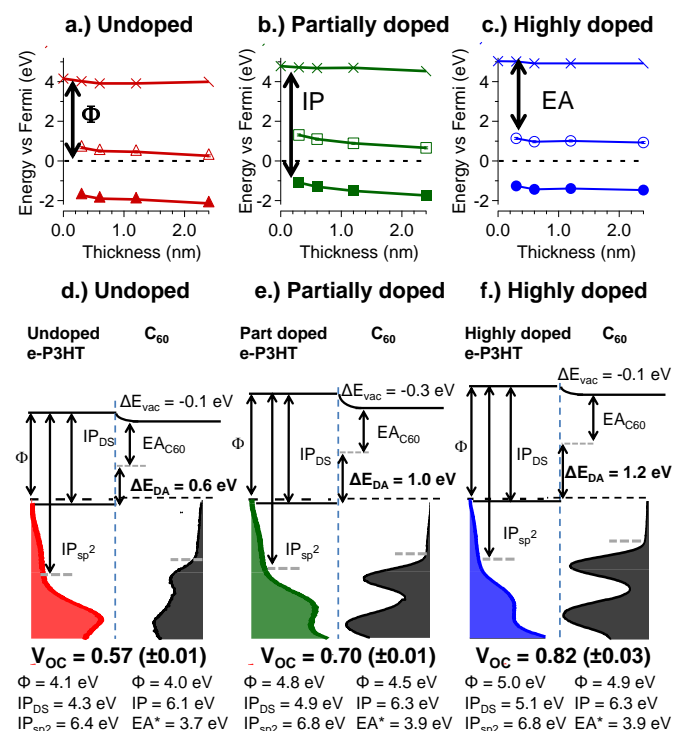
Figure 7. Changes in the work function, onset density of occupied states (IP), and assumed unoccupied states (EA), as a function of increasing C_{60} thickness for the a.) undoped; b.) partially doped, and c.) highly doped e-P3HT film. UPS spectra for each interface and C_{60} thickness are given in the SI section. The electron affinity for C_{60} is estimated using the 2.4 eV band gap determined by Guan et al.[1c, 1d] using IPES. Energy band diagrams inferred from 2.4 nm of C_{60} on d.) undoped, e.) partially doped, and f.) highly doped e-P3HT. The energetic difference between the lowest unoccupied states of the acceptor (C_{60}) and the highest occupied states of the donor (e-P3HT) is given by ΔE_{DA}. ΔE_{DA} is calculated as the difference between the onset of defect states of the e-P3HT (IP_{DS}) and the inferred electron affinity of the C_{60} (EA_{C60}). This value represents the maximum possible open circuit voltage for organic solar cells using these planar heterojunctions as active layers.

A smaller overall change in the percentage of oxidized species with increasing C_{60} thickness was observed for the partially doped film in XPS; the resulting energetics of the C_{60} film show less n-type character (larger energetic difference between the Fermi level and the electron affinity in Figure 7b). There is also a difference in the shift in the vacuum level (indicated as ΔE_{vac}

in Figures 7a and 7b), ranging from -0.1 eV to - 0.3 eV for the undoped and partially doped films, respectively.

Finally, we observed in Figure 5 that the highly doped e-P3HT lost some oxidized character with increasing C_{60} thickness. This could occur from the transfer of an electron from the C_{60} into the polymer, resulting in the energetics of the C_{60} being less n-type. This hypothesis is consistent with the largest separation between the onset density of occupied states and the Fermi level for the C_{60} film, as observed in Figure 7c. Given that no further changes in energetics are observed at fullerene thicknesses greater than 2.4 nm, we conclude that partial electron transfer occurs and is confined near the e-P3HT/C_{60} interface (thickness ~ 1 nm).

Figures 7d-7f show the interpreted energy diagrams, using the UPS spectra for the polymer-only (left side) and 2.4 nm of C_{60} on each polymer (right side). The energetic difference between the unoccupied states of the acceptor (C_{60}) and the occupied states of the donor (e-P3HT) is given by ΔE_{DA}. ΔE_{DA} was determined specifically as the difference between the electron affinity of the C_{60} and the ionization potential of the defect states (IP_{DS}) of the polymer, as a function of oxidation of the polymer system *after* 2.4 nm of C_{60} were deposited onto the e-P3HT films. This energetic difference increases as a function of polymer doping from 0.6 eV for the undoped film to 1.0 eV for the partially doped e-P3HT, and finally, 1.2 eV for the highly doped e-P3HT film. Given that the parameter ΔE_{DA} represents the maximum achievable open circuit voltage when these planar heterojunctions are used as active layers in photovoltaics, we expect that the changes in ΔE_{DA} and the interfacial density of states distributions resulting from charge redistribution may affect the realized V_{OC} in these devices by changing the driving force for charge transfer and by affecting the local energetic dispersions of the interfacial polymer and fullerene species. An increase in V_{OC} from 0.6 V for the undoped polymer to 0.8 V for the highly doped polymer was observed for this system (SI1).

Conclusions

In this work, the variable fraction of oxidized polymer was used to control charge redistribution at the e-P3HT/C_{60} interfaces. Electrochemical oxidative doping of the e-P3HT makes it possible to control the local density of states, which in turn tunes the polymer work function and ionization potential. When the fraction of oxidized species is high, the energetic density of occupied polymeric states near energetically near the unoccupied C_{60} states is low, making charge redistribution improbable. However, charge redistribution from the polymer to the fullerene is more likely in the undoped and partially doped polymer films because they are more electron-rich than the highly doped film, likely resulting in more occupied polymer states poised energetically for charge transfer into the C_{60}.

Because these charge transfer events are localized at the D/A interface, the observed charge redistribution has larger implications for organic electronics such as OPVs. When constructing type II heterojunctions for OPVs, materials are chosen by their bulk properties such as IP_D, EA_A, the resulting ΔE_{DA}, and carrier mobilities. We show that the differences in ionization potentials that result from changes in the polymer p-doping level can have an impact on the energy level alignment between the polymer and the fullerene (ΔE_{DA}), which in addition to controlling interfacial charge redistribution, may also alter kinetic processes such as recombination and generation rates, ultimately impacting the overall device performance.

The key observation in this work is that interfacial charge redistribution at the e-P3HT/C_{60} interface can be controlled by the initial percentage of oxidized polymer as evidenced by the formation of new polaronic species and simultaneous n-doping the C_{60}. Collectively, this work highlights the need to characterize and strategically manipulate localized deviations from bulk properties in the future rational design of functional organic electronics.

Notes and references

* Corresponding author: ratcliff@email.arizona.edu

^a Department of Chemistry and Biochemistry, University of Arizona, 85721

^b Present Address: Department of Chemistry, Eastern Kentucky University, 40475

^c Department of Materials Science and Engineering, University of Arizona, 85721

1. (a) Bredas, J.-L.; Norton, J. E.; Cornil, J.; Coropceanu, V. *Acc. Chem. Res.* **2009,** *42* (11), 1691-1699; (b) Clarke, T. M.; Durrant, J. R. *Chem. Rev.* **2010,** *110* (11), 6736-6767; (c) Guan, Z.-L.; Kim, J. B.; Loo, Y.-L.; Kahn, A. *J. Appl. Phys.* **2011,** *110*, 043719 (4); (d) Guan, Z.-L.; Kim, J. B.; Wang, H.; Jaye, C.; Fischer, D. A.; Loo, Y.-L.; Kahn, A. *Org. Electron.* **2010,** *11* (11), 1779-1785; (e) Heimel, G.; Salzmann, I.; Duhm, S.; Rabe, J. P.; Koch, N. *Adv. Funct. Mater.* **2009,** *19* (24), 3874-3879; (f) Ishii, H.; Sugiyama, K.; Ito, E.; Seki, K. *Adv. Mater.* **1999,** *11* (8), 605-+; (g) Kahn, A.; Zhao, W.; Gao, W. Y.; Vazquez, H.; Flores, F. *Chem. Phys.* **2006,** *325* (1), 129-137; (h) Kanai, Y.; Grossman, J. C. *Nano Lett.* **2007,** *7* (7), 1967-1972; (i) Kawatsu, T.; Coropceanu, V.; Ye, A.; Bredas, J.-L. *J. Phys. Chem. C* **2008,** *112* (9), 3429-3433; (j) Lemaur, V.; Steel, M.; Beljonne, D.; Bredas, J. L.; Cornil, J. *J. Am. Chem. Soc.* **2005,** *127* (16), 6077-6086; (k) Liu, T.; Cheung, D. L.; Troisi, A. *PCCP* **2011,** *13* (48), 21461-21470; (l) McMahon, D. P.; Cheung, D. L.; Goris, L.; Dacuna, J.; Salleo, A.; Troisi, A. *J. Phys. Chem. C* **2011,** *115* (39), 19386-19393; (m) Braun, S.; Osikowicz, W.; Wang, Y.; Salaneck, W. R. *Org. Electron.* **2007,** *8* (1), 14-20; (n) Seki, K.; Ishii, H. *J. Electron. Spectrosc. Relat. Phenom.* **1998,** *88*, 821-830; (o) Tamura, H.; Burghardt, I.; Tsukada, M. *J. Phys. Chem. C* **2011,** *115* (20), 10205-10210; (p) Harris, C.; Kamat, P. V. *Acs Nano* **2009,** *3* (3), 682-690; (q) Huang, J.; Huang, Z.; Yang, Y.; Zhu, H.; Lian, T. *J. Am. Chem. Soc.* **2010,** *132* (13), 4858-4864; (r) Osikowicz, W.; de Jong, M. P.; Salaneck, W. R. *Adv. Mater.* **2007,** *19* (23), 4213-+.

2. Cahen, D.; Kahn, A. *Adv. Mater.* **2003,** *15* (4), 271-277.

3. (a) Ratcliff, E. L.; Jenkins, J. L.; Nebesny, K.; Armstrong, N. R. *Chem. Mater.* **2008,** *20* (18), 5796-5806; (b) Ratcliff, E. L.; Lee, P. A.; Armstrong, N. R. *J. Mater. Chem.* **2010,** *20* (13), 2672-2679; (c) Ratcliff, E. L.; Zacher, B.; Armstrong, N. R. *J. Phys. Chem. Lett.* **2011,** *2* (11), 1337-1350.

4. Mehraeen, S.; Coropceanu, V.; Bredas, J.-L. *Phys. Rev. B: Condens. Matter* **2013,** *87* (19) 195209.

5.   (a) Brumbach, M.; Veneman, P. A.; Marrikar, F. S.; Schulmeyer, T.; Simmonds, A.; Xia, W.; Lee, P.; Armstrong, N. R. *Langmuir* **2007,** *23* (22), 11089-11099; (b) Marrikar, F. S.; Brumbach, M.; Evans, D. H.; Lebron-Paler, A.; Pemberton, J. E.; Wysocki, R. J.; Armstrong, N. R. *Langmuir* **2007,** *23* (3), 1530-1542.

6.   Heinze, J.; Rasche, A.; Pagels, M.; Geschke, B. *J. Phys. Chem. B* **2007,** *111* (5), 989-997.

7.   Kim, Y.; Cook, S.; Tuladhar, S. M.; Choulis, S. A.; Nelson, J.; Durrant, J. R.; Bradley, D. D. C.; Giles, M.; McCulloch, I.; Ha, C. S.; Ree, M. *Nat. Mater.* **2006,** *5* (3), 197-203.

8.   (a) Skompska, M.; Szkurlat, A. *Electrochim. Acta* **2001,** *46* (26-27), 4007-4015; (b) Skompska, M.; Szkurlat, A.; Kowal, A.; Szklarczyk, M. *Langmuir* **2003,** *19* (6), 2318-2324.

9.   Reid, O. G.; Rumbles, G. *J. Phys. Chem. Lett.* **2013,** *4* (14), 2348-2355.

10. (a) Liang, Z.; Gregg, B. A. *Adv. Mater.* **2012,** *24* (24), 3258-3262; (b) Liang, Z.; Reese, M. O.; Gregg, B. A. *ASC Appl. Mater. Inter.* **2011,** *3* (6), 2042-2050.

11. (a) Ayzner, A. L.; Tassone, C. J.; Tolbert, S. H.; Schwartz, B. J. *J. Phys. Chem. C* **2009,** *113* (46), 20050-20060; (b) Bai, X.; Holdcroft, S. *Macromolecules* **1993,** *26* (17), 4457-4460; (c) Banerji, N.; Seifter, J.; Wang, M.; Vauthey, E.; Wudl, F.; Heeger, A. J. *Phys. Rev. B: Condens. Matter* **2011,** *84* (7) 075206; (d) Ohkita, H.; Cook, S.; Astuti, Y.; Duffy, W.; Tierney, S.; Zhang, W.; Heeney, M.; McCulloch, I.; Nelson, J.; Bradley, D. D. C.; Durrant, J. R. *J. Am. Chem. Soc.* **2008,** *130* (10), 3030-3042.

12. (a) Paquin, F.; Latini, G.; Sakowicz, M.; Karsenti, P.-L.; Wang, L.; Beljonne, D.; Stingelin, N.; Silva, C. *Phys. Rev. Lett.* **2011,** *106* (19) 197401; (b) Reid, O. G.; Malik, J. A. N.; Latini, G.; Dayal, S.; Kopidakis, N.; Silva, C.; Stingelin, N.; Rumbles, G. *J. Polym. Sci., Part B: Polym. Phys.* **2012,** *50* (1), 27-37.

13. (a) Owens, D. W.; Aldao, C. M.; Poirier, D. M.; Weaver, J. H. *Phys. Rev. B: Condens. Matter* **1995,** *51* (23), 17068-17072; (b) Yang, S. H.; Pettiette, C. L.; Conceicao, J.; Cheshnovsky, O.; Smalley, R. E. *Chem. Phys. Lett.* **1987,** *139* (3-4), 233-238; (c) Matz, D. L.; Ratcliff, E. L.; Meyer, J.; Kahn, A.; Pemberton, J. E. *ASC Appl. Mater. Inter.* **2013,** *5* (13), 6001-6008.

14. Castet, F.; D'Avino, G.; Muccioli, L.; Cornil, J.; Beljonne, D. *Physical chemistry chemical physics : PCCP* **2014,** *16* (38), 20279-90.